

INTERNATIONAL CLIMATE INITIATIVE

Regional project
Climate Protection through Forest Conservation
in Pacific Island Countries

On behalf of



Federal Ministry for the
Environment, Nature Conserv
and Nuclear Safety

of the Federal Republic of Germany

**SAR-based Deforestation Assessment,
Espiritu Santo Island, Vanuatu**

Processing description and results
Version 1.0

January, 18 2013



SPC
Secretariat
of the Pacific
Community



SPC Land Resources Division



Deutsche Gesellschaft
für Internationale
Zusammenarbeit (GIZ) GmbH



Prepared by: **mesa consult**

On behalf of SPC/GIZ Regional Project
“Climate Protection through Forest
Conservation in Pacific Island Countries”

P.O. Box 14041, SUVA, Fiji

e-mail: karl-peter.kirsch-jung@giz.de

Table of content

Introduction.....	4
1. Earth observation data description	5
2. Detecting forest cover change using the γ^0 backscatter coefficient.....	6
3. Overview over the processing chain.....	7
4. Processing steps	9
Step 1: image registration	9
Step 2: FLS masking.....	11
Step 3: Speckle reduction	12
Step 4: Conversion to radar cross section	14
Step 5: Mosaicking.....	14
Step 6: Zonal statistics	14
Step 7: Deforestation detection	15
Step 8: Deforestation masking	16
Step 9: Deforestation pattern assessment.....	17
Step 10: Accuracy Assessment.....	20
5. Recommendations to improve the processing chain.....	21
References	23
Acronyms	24
Annex 1: Header file content for tiles S15E166 and S15E67	25
Annex 2: HV forest sampling design.....	26
Annex 3: Accuracy assessment sampling design.....	27

Introduction

Reducing emissions from deforestation, forest degradation, sustainable management of forests, enhancement and conservation of forest carbon stocks (REDD+) is considered one of the most cost-effective options to mitigate climate change. The Conference of the Parties (COP) of the United Nations Framework Convention on Climate Change (UNFCCC) frames REDD+ as one of the building blocks of the post-Kyoto mitigation architecture negotiated in the Ad-hoc Working Group on Long-term Cooperative Action (AWG-LCA) and The Subsidiary Body on Scientific and Technological Advice (SBSTA). While Parties haven't yet concluded on measurement, reporting and verification (MRV) of greenhouse gas emission reductions and Removals (ERR), the modalities for establishing reference (emission) levels and for informing on safeguards compliance have been agreed. The Cancún-Agreements frame REDD+ implementation as a phased approach: Countries are requested to develop their REDD+ strategies or action plans to defined policies to be implemented in the second phase involving capacity building, technology development and results-based demonstration activities, evolving into results-based actions that should be fully measured, reported and verified during the third phase (1/CP.16 par. 73 in FCCC/CP/2010/7/Add.1).

With support of the SPC/GIZ Regional Project "Climate Protection through Forest Conservation in the Pacific Island Countries", Vanuatu is currently developing its Readiness Preparation Proposal (R-PP) to the Forest Carbon Partnership Facility (FCPF) of the World Bank. The Government of Vanuatu and GIZ agreed to develop REDD+ building on subnational approaches and to pilot the national REDD+ mechanism on Santo Island. As outlined in the RPP, the deforestation monitoring will partially build on Synthetic Aperture Radar (SAR) Technology, which is particular suitable to detect land cover and land use in clouded regions. Together with GIZ Philippines, the SPC/GIZ Regional Project participates in the 3rd Kyoto and Carbon (K&C 3) Science Program of the Japan Aerospace Exploration Agency (JAXA). Within this program, Vanuatu is granted access to pre-processed SAR data of the ALOS Palsar sensor and technical training in deforestation detection.

This document describes the steps to derive the 2007 – 2010 deforestation patterns for Espiritu Santo Island processing ALOS Palsar data. Section 1 introduces the data sets. Section 2 presents the approach how to detect forest cover change based on the gamma naught (γ^0) backscatter coefficient. While section 3 provides an overview over the processing chain as a whole, section 4 describes each processing step in detail. Section 5 discusses potential limitations due to data and processing constraints and provides guidance how to improve the assessment.

1. Earth observation data description

The 2007 – 2010 deforestation analysis for Santo Island is based on 3 data sets:

- ALOS Palsar fine resolution model dual polarization (FBD) L-band Synthetic Aperture Radar data has been processed to detect the deforestation.
- World View 2 from 2011 data has been used as a source to validation the patterns and assess their geometric and thematic accuracy.
- The NEXTMap® TopoSAR Digital Surface Model (DSM) of the Vanuatu Department of Lands and Survey provided an additional very-high resolution reference for the coastline and geometric accuracy of the SAR data.

Within the K&C3 science program, JAXA distributes the ALOS Palsar FBD data at a special processing level and format: The data comes as a 25m spatial resolution ortho-rectified and slope corrected mosaic product composed of tiles organized along the geographic latitudes and longitudes of the World Geodetic System (WGS), in equal rectangular map projection. Each tile is a composite of 5 files: the header file providing the metadata following the format established by JAXA (JAXA 2012a), two file files providing the horizontal-horizontal (HH) and horizontal-vertical (HV) polarization data, a mask file indicating areas suffering from geometric and radiometric distortions due to several radar specific effects (e.g., foreshortening, range and azimuth shift, layover, radiometric variation due to the slope, and shadowing), a file providing the calculated local incidence angle of the backscatter signal based on slopes derived from the Shuttle Radar Topography Mission (SRTM) Digital Surface Model (Shimada 2010), and a file indicating the acquisition date of each part forming the tile. HH and HV data has already passed radiometric normalization (range spreading loss correction, antenna pattern gain correction, and incidence angle correction). Being ortho-rectified and slope corrected, the K&C 3 data differs from standard ALOS Palsar processing levels (Level 1.1 and 1.5) and formats (JAXA 2008). Its geometric accuracy depends on the geometric accuracy of the DSM (SRTM: 90m) having been used in slope correction and ortho-rectification.

To provide a very-high resolution source for accuracy assessment and coconut palm stand delineation, GIZ acquired a WorldView 2 multispectral (1.84 m resolution) and panchromatic (0.46 m) data set covering Santo Island. Its image tiles have been acquired between March 2010 and June 2011. A combination of Band 7 (Red-Edge: 705-745 nm), 5 (Red: 630-690 nm), and 2 (Blue: 450-510 nm) has been used for visual assessment of the thematic and geometric accuracy.

The NEXTMap® TopoSAR Ortho-rectified Radar Image (ORI) set has been commissioned by Vanuatu's Department of Lands and Survey as a basis for a revised national topographic map. One of its by-products is a 5m DSM which has been used to derive the coast lines of Santo Island to assess the geometric accuracy of the SAR data. The following section describes how the data has been used in the processing chain.

2. Detecting forest cover change using the γ^0 backscatter coefficient

The backscatter intensity of the radar signal depends on the radar system parameters (polarization, depression angle, wavelength) and the properties of the target on the ground (dielectric constant (moisture content), surface roughness, local geometry and shape of the object, (Lusch 1999)). Differences in the intensity of the radar backscatter signal captured by different backscatter coefficients can be used to detect land-use change (Lee and Pottier 2009; Shimada 2010). JAXA has developed a set of processing routines in form of shell scripts to detect forest cover change applying the PALSAR gamma naught (γ^0) backscatter coefficient to the HV polarization (JAXA 2012b).

Backscatter coefficients are derived solving the fundamental radar equation (Lusch 1999):

$$(1) \quad P_R = P_T(\sigma^0 A) \left[\frac{G^2 \lambda^2}{(4\pi)^3 R^4} \right]$$

where: P_R = the power returned to the radar antenna by an extensive target

from: P_T = the power transmitted by the radar system

σ^0 = the radar scattering coefficient of the target

A = area of the resolution cell of the radar

System: G = gain of the antenna

λ = wavelength of the radar system

R = range from the antenna to the target

As the intensity of the backscatter signal is modulated by the terrain (cf. figure 1), backscatter coefficient have to be normalized anticipating the geometry of the radar illumination area (Shimada 2010) captured by the local incident angle θ . Gamma naught (γ^0) gives the backscatter per unit area of the incident waveform (red line) perpendicular to slant range (dotted black line). It is defined as (equation 2):

$$(2) \quad \gamma^0 = \sigma^0 / \cos\theta$$

Calibrating the HV processing

Figure 1: Influence of the Incident Angle θ

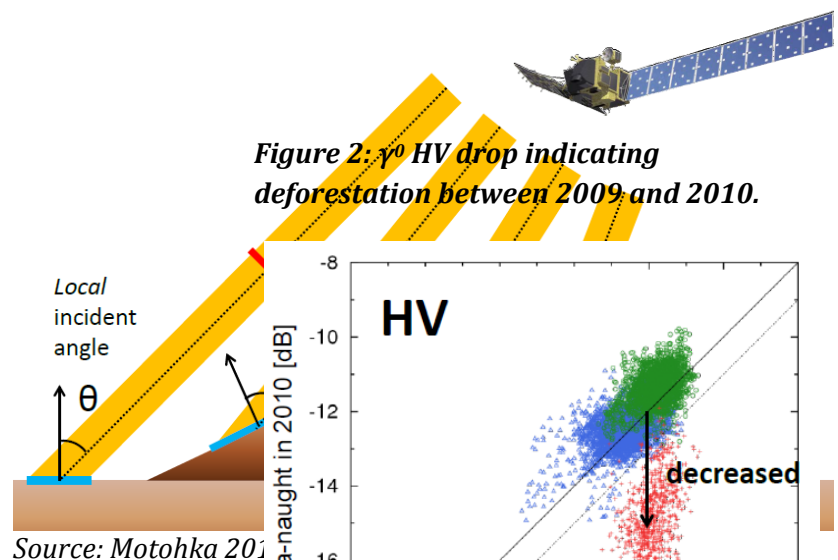
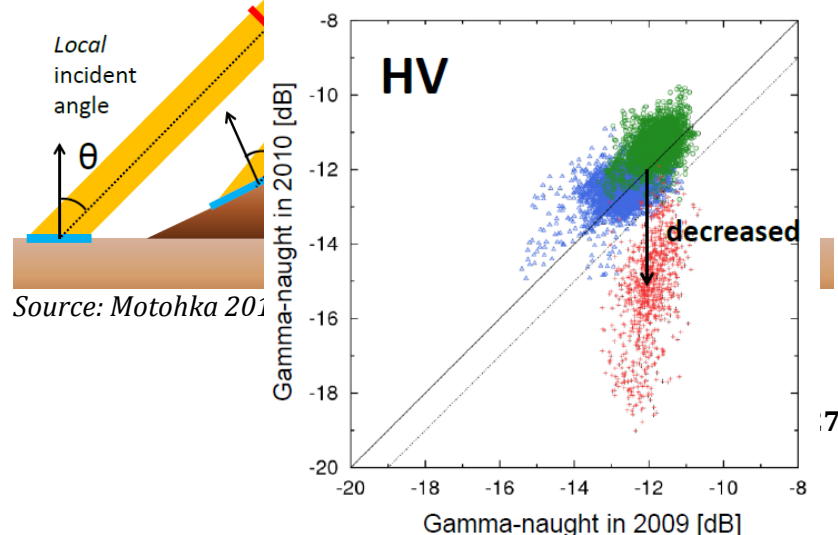


Figure 2: γ^0 HV drop indicating deforestation between 2009 and 2010.



Source: Motohka 2012

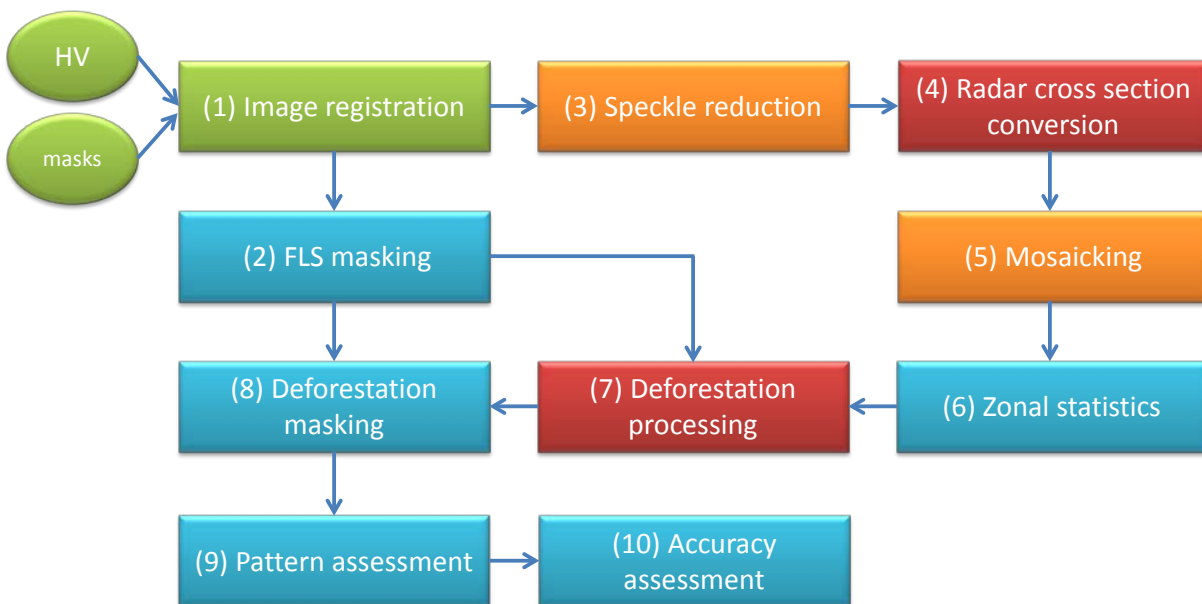
with field observations provides a way to detect deforestation for specific forest ecosystems (Motohka 2012). As the scatterplot in figure 2 illustrates, a decrease (red) of the γ^0 HV backscatter of natural forest (green) and acacia plantations (blue) indicates a change from forest to non-forest during 2009 to 2010. As moisture content over canopy varies across seasons, suitable threshold values needs to be determined to distinguish forest cover change from seasonal variability (Isoguchi 2012). However, this approach can only indicate where land cover change occurred. It requires *a priori* knowledge about the location of intact forest to define a backscatter signal range representing forest ecosystems to qualify land cover change as deforestation. The following section outlines the processing chain to detect deforestation applying this approach.

3. Overview over the processing chain

Standard SAR processing includes several steps to convert the backscatter signal into thematic information starting with geocoding and image registration, moving to radiometric normalization, speckle reduction, edge enhancement, conversion into radar cross section, derivation of thematic descriptors, radiometric adjustment, and classification (Leica Geosystems 2006). As mentioned, the K&C 3 ALOS Palsar FBD data has passed radiometric normalization, ortho-rectification and slope correction. JAXA developed two alternative processing chains, one relying on the availability of forest-/non-forest cover maps for each year to be processed, and a modified processing chain generating calibration data to identify the backscatter range of forests as part of the processing. As the forest-/non-forest cover maps for Santo Island haven't been processed, so far, the second approach is being applied with some modifications which are explained in detail in section 4.

Figure 3 outlines the processing chain: (1) All necessary file (HV polarization, mask file) were registered according to their relative geographic position. (2) While the radar signal is capable of penetrating clouds, it comes with the disadvantage that certain geometric constellations of the radar signal in relation to the topography lead to geometric and radiometric distortions (FLS: foreshortening, layover, range and azimuth shift, radiometric variation due to the slope, and radar shadowing) which have to be masked out. (3) Variation of the backscatter causes signal noise (speckle) which has to be reduced applying suitable filter techniques. (4) Then, the amplitude data has to be converted to normalized radar cross section data (in decibels). (5) To detect suitable thresholds excluding seasonal variation HV applicable to the whole island, mosaics were created

Figure 3: γ^0 -based processing chain



for each year (2007, 2010). (6) Based on a systematic sampling scheme, relevant threshold values were determined to detect the backscatter range for forests using zonal statistics (mean backscatter and standard deviation). (7) The statistical parameters were factored into JAXA's shell script processing land cover change for the backscatter range established by the parameters. (8) As these ranges are only meaningful for areas without geometric or radiometric signal distortion, changes in distorted areas were masked out applying the results of step 2. Finally, the plausibility and consistency of the detected deforestation patterns (9), and the thematic accuracy of the final results (10) have to be assessed.

While step 1 has been performed using a standard text editor, steps 3 and 5 were implemented in the Next ESA SAR Toolbox (NEST 4C-1.1) an open source software provided by the European Space Agency¹. Steps 4 and 7 were performed using JAXA's shell scripts. All other steps ((2), (6), (8)-(10)) were implemented in ArcGIS 10.0. The next section describes the steps in detail.

¹ NEST 4C-1.1 is available at: <http://nest.array.ca/web/nest>.

4. Processing steps

Step 1: image registration

K&C data is distributed as raw data requiring the appropriate format and map projection to be established by a header file (text file with *.hdr extension). The 3² tiles covering Espiritu Santo Island are named S14E166, S15E166, and S15E167. The name is a composite of the upper left latitude and longitude of each tile. To register the tiles correctly, the file format of each of the 5 files (HH/HV, mask, incident, acquisition date) has to be considered. Table 1 gives the scene parameters for each type (all types follow BSQ interleave).

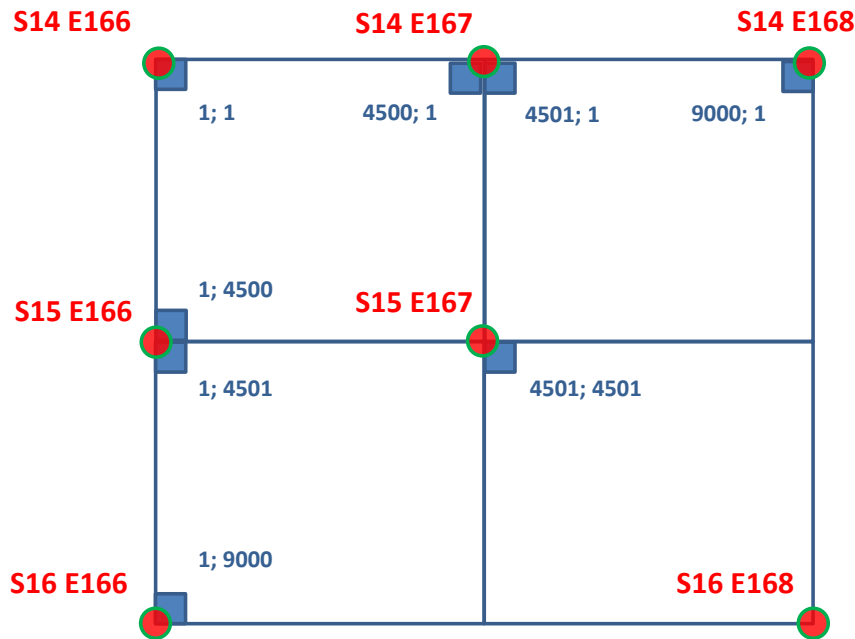
Table 1: Scene format parameters

File Type	File Type	Scene size: col, lines	Data type
Image Files: HH & HV	16 bit unsigned short	4500, 4500	Unsigned int
Mask File	8 bit unsigned short	4500, 4500	Byte
Incidence Angle File	8 bit unsigned short	4500, 4500	Byte
Acquisition Date File	16 bit unsigned short	4500, 4500	Unsigned int

The files follow an equal rectangular map projection. Figure 4 illustrates the internal and external geo-reference of the tiles. The upper left corner of the upper left pixel of tile S14E166 has the geographic coordinates Lat.: -14.00, long 166.00. The internal coordinates of the pixel are 1; 1.

² A small part of the northeastern part of Santo Island is being covered by tile S14E167 which hasn't been processed, so far. I will be included in an update of this report.

Figure 4: Internal and external map reference of the tiles



To facilitate the registration, an ENVI header file for each of the 5 files covering one tile can be created using a standard text editor. The header file has to be named in the same way as its corresponding data file extended by an *.hdr. The following example shows the content of the file S14E166_07_sl_HV.hdr:

```

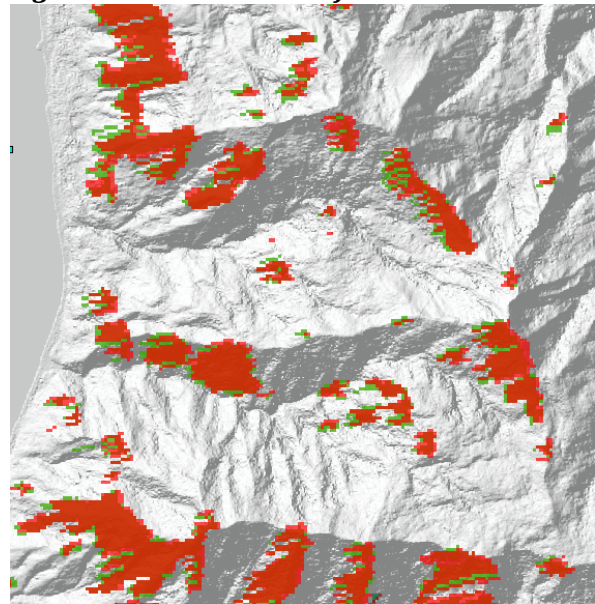
ENVI
description = {
  File Imported into ENVI.}
samples = 4500
lines = 4500
bands = 1
header offset = 0
file type = ENVI Standard
data type = 12
interleave = bsq
sensor type = Unknown
byte order = 0
map info = {Geographic Lat/Lon, 1.0000, 1.0000, 166.00000000, -14.00000000, 2.2222000000e-004,
2.2222000000e-004, WGS-84, units=Degrees}
coordinate system string =
{GEOGCS["GCS_WGS_1984",DATUM["D_WGS_1984",SPHEROID["WGS_1984",6378137.0,298.25722356
3]],PRIMEM["Greenwich",0.0],UNIT["Degree",0.0174532925199433]]}
wavelength units = Unknown
    
```

The same header file content can be used for the files S14E66_XX_sl_HH and S14E66_XX_sl_date (XX stands for different years, e.g. 07: 2007, 10: 2010). The header file for the incidence angle and mask require one single adjustment in line 9 setting the data type to “1”. Annex 1 provides the header file content for the two tiles S15E166 and S15E67.

Step 2: FLS masking

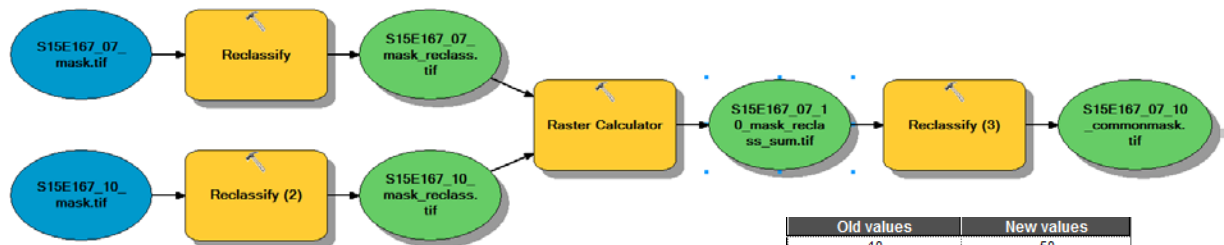
Rough terrain causes geometric and radiometric distortions in the radar image (Lusch 1999; Lee and Pottier 2009; Shimada 2010). As the geometric distortions, caused by foreshortening, layover, and radar shadowing (FLS), depend on the topography and the antenna look angle, the geometric distortions have to be masked out for each image and year. Even if the look angle doesn't change, image specific masking is required, as slight changes of the antenna position cause variations of the distortions on the ground. Figure 5 illustrates this effect indicating FLS distortions for 2007 (green) and 2010 (red) as overlays over the 5m DSM. Figure 7 shows the location of the area.

Figure 5: FLS distortions for 2007 and 2010



To capture all distortions, the mask files for each tile and year were merged by reclassifying the mask of each tile, combining them into one (“SUM”) and reclassifying the result to the original classification scheme. The result allows to derive a common land (value: 255)-sea (value: 50) mask for each tile³. Figure 6 shows the steps and configuration of the reclassification process.

Figure 6: Processing of the common FLS mask for 2007 and 2010 for tile S15E167



Old values	New values
0	0
50	10
100	100
150	1000
255	10000
NoData	NoData

Sea
FLS
FLS
Land

Old values	New values
10	50
20	50
100	100
110	50
160	50
200	100
1000	150
1100	100
2000	150
10010	50
10100	100
11000	150
20000	255
NoData	NoData

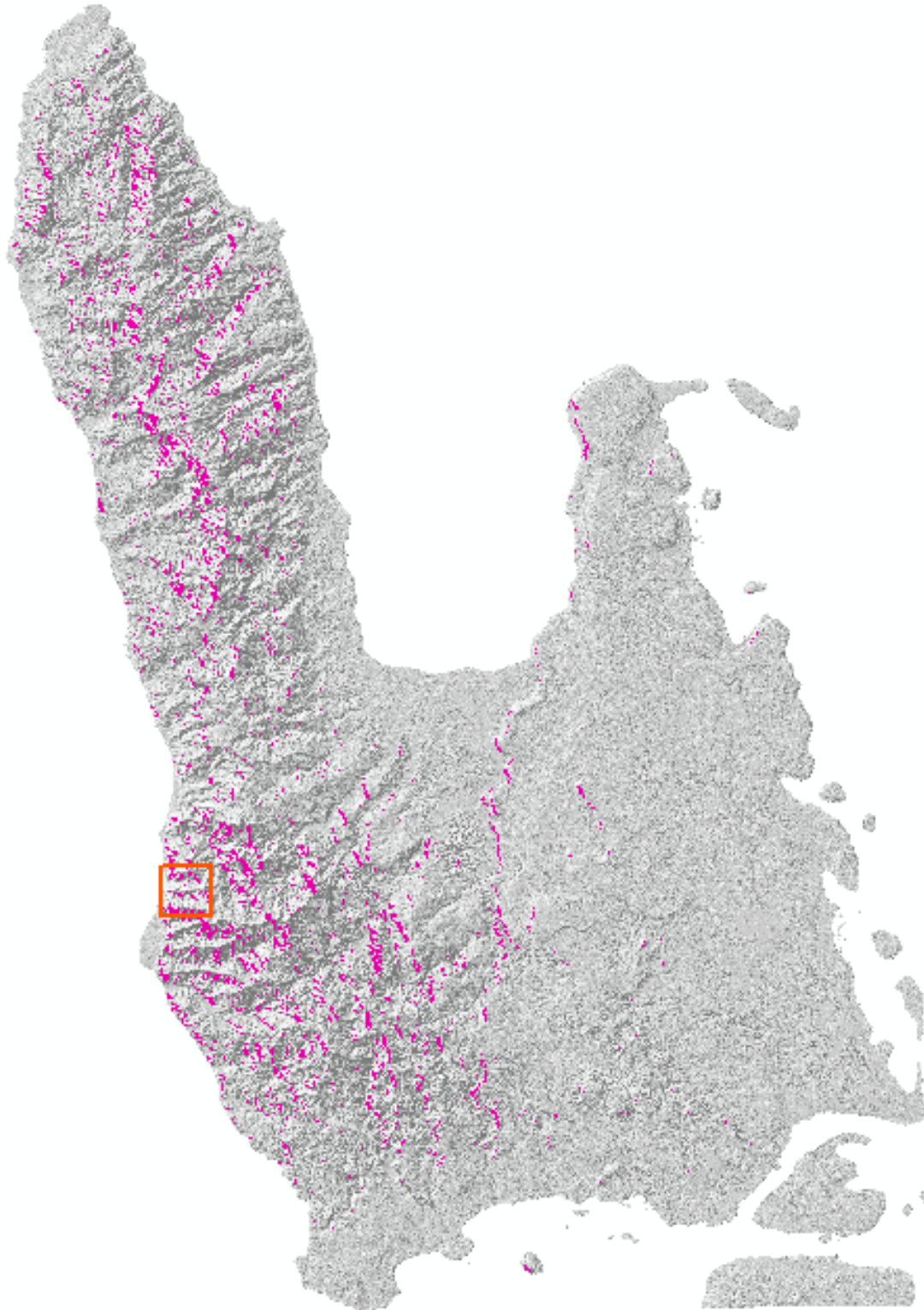
Using a combined FLS mask in the processing represents a deviation from JAXA's processing chain which includes the 2010 mask only. However, the combined mask avoids erroneous results in areas, which appear inside the 2007mask, but outside the 2010 mask.

Figure 7 presents the result of masking process as an overlay over the 5m DSM. The rough topography of Santo's west coast causes numerous FLS distortions, mostly on steep slopes oriented towards the south and southeast. Overall, 3.1% of Santo's land mask are affected by FLS distortions and have to be excluded from radar processing. However, land cover in the areas masked-out can be visually interpreted using WorldView-2 data.

Step 3: Speckle reduction

Local constructive and destructive interferences between the radar signal and the target's surface cause noise in the backscatter signal. Averaging the backscatter across a defined domain applying specific filter techniques reduces speckle, and enhances radiometric resolution, although at the expense of spatial resolution (Natural Resources Canada 2007). A 3x3 Lee filter was applied to the HV polarization to moderately reduce speckle.

Figure 7: Merged 2007 2010 FLS mask (purple) and location of figure 5 (orange)



Step 4: Conversion to radar cross section

As SAR data is being distributed as amplitude data, the digital numbers (DN) need to be converted to normalized radar cross section (NRCS) in decibels [db] applying a sensor specific Calibration Factor (CF):

$$(3) \sigma^0 = 10 \log_{10}[DN^2] * CF$$

With: CF = - 83.0 db (JAXA 2012a).

Step 5: Mosaicking

To generate the inputs for step 6: Zonal statistics, HV mosaics of the three tiles for each year (2007, 2010) were created using NEST 4V-1.1.

Step 6: Zonal statistics

JAXA's processing chain requires the determination of two forest specific parameters

Ave_{YYYY}: The average HV value representing forest for each year YYYY;

St_{YYYY}: The standard deviation of the average HV value representing forest for each year YYYY;

While JAXA recommends determining these parameters using one sample per tile, we have opted for a systematic sampling approach covering all forests of Santo Island. A sampling population was established generating a regular grid of 1x1km square plots using the Geospatial Modeling Environment GME 0.7.2 (Beyer 2012)⁴. From this population all square samples were selected which are completely within the 2000 forest mask developed by Herold et al. (2007). The spatial selection yielded 135 samples which were visually inspected overlaying them over corresponding WorldView 2 2011 scenes. 73 plots completely covered by forest cover in 2011 were selected as samples to calculate the average forest HV backscatter and its corresponding standard deviation for the years 2007 and 2010 applying zonal statistics to the mosaics created in step 5. Annex 2 shows the distribution of the sampling plots and table 2 presents the parameters for each year. Parameter values for forest were used to calibrate the deforestation detection.

Table 2: Parameters determining the forest definition

Year	State of forest	MIN [db]	MAX [db]	RANGE [db]	MEAN [db]	STD
2007	completely covered	-24.434379	-6.682885	17.751493	-12.563281	1.448516
	partially covered	-22.622583	-1.508473	21.114110	-12.271896	1.371590
2010	completely covered	-21.910715	-6.191668	15.719045	-12.384159	1.429186
	partially covered	-21.796533	-0.595594	21.200939	-12.253571	1.318547

⁴ GME is freely available at: <http://www.spatalecolology.com/gme/>. The current version still has dependencies on R (R Core Team 2012) and ArcGIS 10.x.

Step 7: Deforestation detection

Empirical tests showed that the seasonal HV variation due to moisture content over canopy can reach 0.5 db, while 2-3 db decreases in the HV signal can be attributed to a decrease of volume scattering indicating change from forest to non-forest (Isoguchi 2012). JAXA's algorithm for the deforestation detection without annual forest-/non-forest masks performs the following steps:

(1) Calculation of the 2007 - 2010 HV differential images: JAXA's algorithm receives the 2007 and 2010 HV images as well as the corresponding mask files as an input. Deviating from the JAXA's approach, the masks files were replaced by the combined 2007-2010 mask files generated in step 10. The algorithm calculates the 2007 - 2010 HV differential image for each tile masking out sea and water bodies. Equation 4 provides the map algebra expression for tile S15E167:

$$(4) [S15E167_{10} - 07_{diff}] = [S15E167_{10_sl_HV}] - [S15E167_{07_sl_HV}]$$

(2) Decision tree analysis to detect forest and non-forest: The script calculates the delta factor Δ representing a bias between two corresponding scene as follows:

$$(5) \Delta = Av_{2010} - Av_{2009}$$

The delta factor is being used to define a threshold (threshd1) for inter-annual HV variations:

$$(6) \text{threshd1} = \text{user_defined1} + \Delta$$

With: $\text{user_defined_1} = -1$ db (The parameter value can be adjusted in the `mk_diff_mosaic.prm` file).

The script increases the threshold value and calculates the corresponding results to assess their sensitivity to the threshold value:

$$(7) \text{threshd2} = \text{threshd1} - 2.0$$

$$(8) \text{threshd3} = \text{threshd1} - 4.0$$

If the value of a certain pixel in the differential map remains below threshd1, the pixel flags land cover change (LCC: change exceeding seasonal variability or inter-annual bias).

$$(9) [S15E167_{10} - 07_{diff}] = \begin{cases} \text{LCC}, [S15E167_{10} - 07_{diff}] < \text{threshdx} \\ \neg\text{LCC}, [S15E167_{10} - 07_{diff}] \geq \text{threshdx} \end{cases}$$

To identify deforestation (HV changes exceeding a certain threshold) within land cover change, the algorithm uses the four parameters determined in step 6 ($Ave_{2007, 2010}$; $Stv_{2007, 2010}$) which have to be handed over to the shell script when initiating it. It calculates the potential forest domain for each tile and year using the average HV backscatter for each year (Ave_{YYYY}) and a multiple standard deviation (Stv):

$$(10) \text{Forest}_{YYYY} = [(Av_{YYYY} + (\text{user_defined2} * Stv_{YYYY})); (Av_{YYYY} - (\text{user_defined2} * Stv_{YYYY}))]$$

With: user_defined_2 = 2.0 (The parameter value can be adjusted in the mk_diff_mosaic.prm file).

If a pixel is flagged as a change candidate (equation (9)), the algorithm assesses whether it has been covered by forest in year 2007 and is covered by non-forest in 2010. If the changed pixel appeared to be forest in 2007 and non-forest in 2010, it is classified as deforestation; else it is flagged as non-forest. Figure 8 introduces the console output of the shell script for tile S15E167.

Figure 8: Script output for tile S15E167

```
#####
Process making difference image and gamma0 change map
#####
[ Make different image and gamma0 change map ]
c:/JAXA/GCMap_Training/data/S15E167_10_sl_HV average = -12.384160
c:/JAXA/GCMap_Training/data/S15E167_10_sl_HV stdev = 1.429186
c:/JAXA/GCMap_Training/data/S15E167_07_sl_HV average = -12.563280
c:/JAXA/GCMap_Training/data/S15E167_07_sl_HV stdev = 1.448516
delta factor = 0.179120
thresd1 = -0.820880
thresd2 = -2.820880
thresd3 = -4.820880
c:/JAXA/GCMap_Training/data/S15E167_10_sl_HV : -15.242532 < dB < -9.525788
c:/JAXA/GCMap_Training/data/S15E167_07_sl_HV : -15.460312 < dB < -9.666248

[ calculate point of change case ]
case1<-2.820880 < diff <= -0.820880> : point=23307, 0.12[%]
case2<-4.820880 < diff <= -2.820880> : point=2969, 0.01[%]
case3< diff <= -4.820880> : point=529, 0.00[%]
all case : point=26805, 0.13[%]

Finished!!!
```

Apart, the shell script generates two maps for each tile: The [tile_name]_10-07_diff -file (data type: 32bit-floating /"data type = 4") provides the HV differences for the land mask, the file [tile_name]_10-07_gcm provides the Gamma naught change map (GCM file type: 8bit-unsigned /"data type = 1"). It indicates the areas flagged as deforested for different threshold intervals:

Table 3: Output classes of the deforestation analysis

Pixel value	Concept
0	water
59	pixels classified as deforested for the range [thresd2; thresd1]
60	pixels classified as deforested for the range [thresd3; thresd2]
61	pixels classified as deforested for the range [< thresd3]
253	Other

At this stage of the processing, the γ^0 change map represents an interim product as the areas subject to geometric and radiometric distortions (FLS) haven't been masked out by the shell script. Consequently, an additional masking process is necessary to exclude those areas.

Step 8: Deforestation masking

To calculate the deforestation between 2007 and 2010, the FLS mask generated in step 2 was reclassified (“07_10_commonmask_land_wo_FLS”) setting sea, FLS areas, and no data to 0, and land to 1. The recoded mask was converted into a shapefile, and the land mass of Santo Island was selected excluding all other islands (“07_10_Santo_landmask”). Using Map Algebra, the deforestation outside the FLS area on Santo island (“07_10_Santo_deforestation.tif”) was calculated (figure 9). Table 4 presents the results of the analysis.

Figure 9: Map Algebra model to exclude FLS area and to extract deforestation on Santo

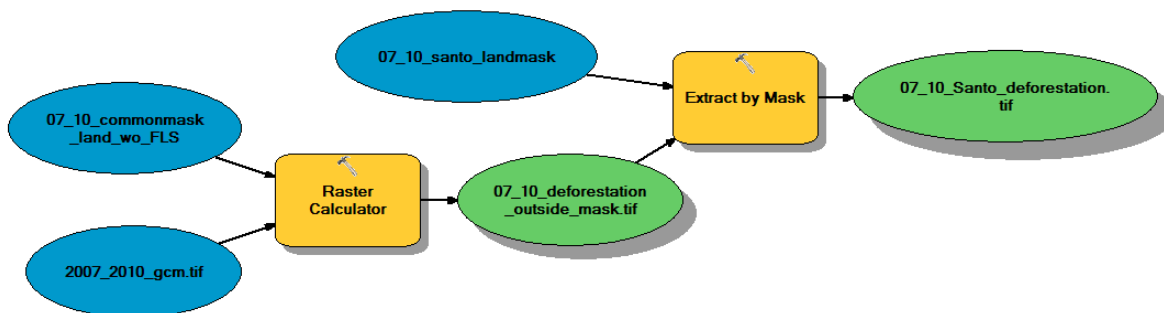


Table 4: 2007 – 2010 deforestation on Santo Island

Class	Code	# Pixel	Area [ha]	% of Total Area
FLS	0	206,989	12,937	3.1
Deforestation [threshd2; threshd1]	59	63,106	3,944	1.0
Deforestation [threshd3; threshd2]	60	9,146	572	0.1
Deforestation [< threshd3]	61	1,084	68	0.0
Land	243	6,355,729	397,233	95.8

According to the results at this stage, 4,584 ha have been deforested during the 3 year period corresponding to an annual deforestation of 1,528 ha/yr. This deforestation rate appears very high compared to a rate of 467.8 ha/yr for the whole of Vanuatu reported for the period 1990 to 2000 (Herold et al. 2007). This discrepancy requires further analysis of the deforestation pattern.

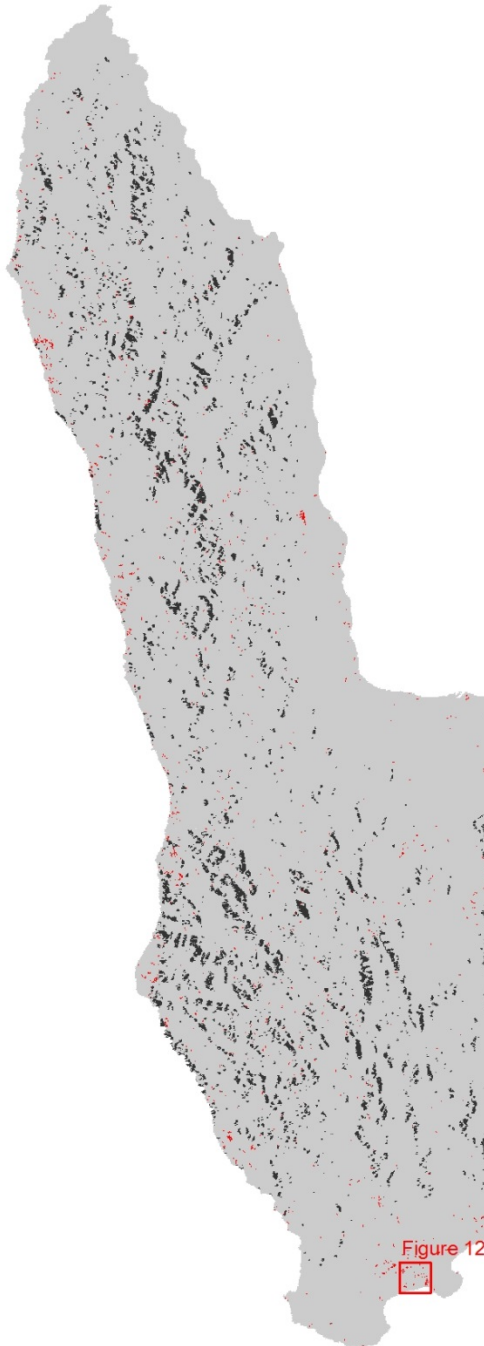
Step 9: Deforestation pattern assessment

The histogram reveals that distribution of the size of deforested areas is extremely skewed. 77% of the total deforestation is attributed to areas smaller than the minimum mapping unit (3x3 pixel \cong 75m x 75m = 0.5625 ha) and has to be excluded as remaining speckle. 1,396.8 ha⁵ or 465.6 ha/yr

⁵ The results are based on vector-based analysis converting the raster file into polygons and re-projecting them to a planar system (UTM58S, WGS 84). The total size of all deforestation polygons reaches 4,305.5 ha, that is 6.1% less than the raster based analysis (table 4) indicates. Despite the error, the polygon based analysis will be used as some of the following analytical steps can be implemented easier in a GIS environment.

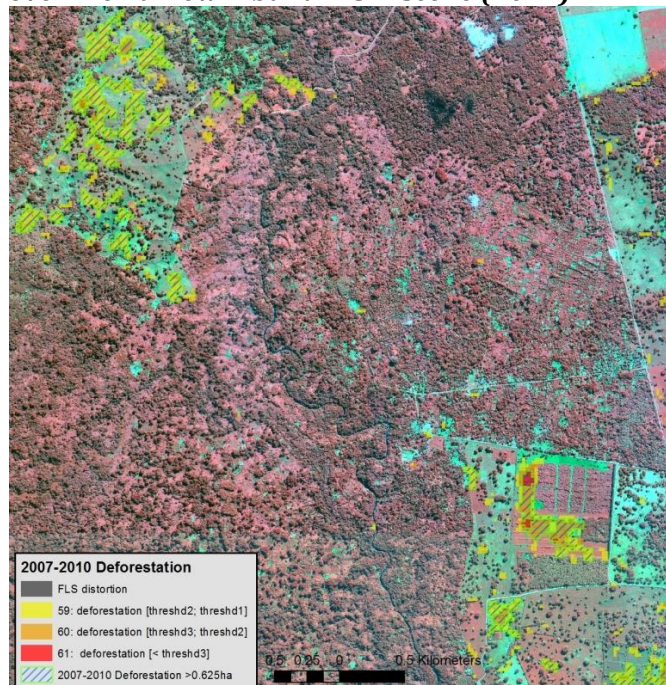
can be reported as a consolidated deforestation rate for the period 2007-2010. Figure 10 presents the distribution of those areas.

Figure 10: Deforestation (> 0.5625 ha) between 2007 and 2010 on Santo Island



The spatial distribution shows, that most of the deforestation occurred in the agricultural area around Santo's capital

Figure 11: Deforestation pattern in the Southeast over WorldView-2 band 7-5-2 scene (2011)



Luganville in the Southeast, between the villages Ipayato and Viase in the Southwest, and in the Northern part of the west coast. Around Luganville, most of the deforestation occurs inside agricultural areas which appear to have been deforested quite some time ago. Here, additional clearing of remaining trees and smaller forest stands might have caused the change in the backscatter signal (figure 11; location shown in figure 10).

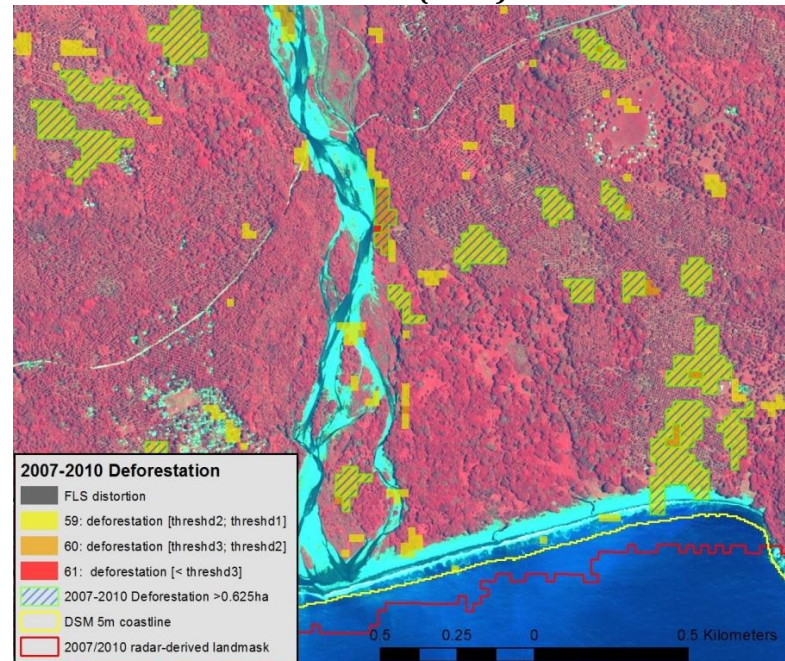
In the Southwest, deforestation patterns are visible within coconut palm stands (figure 12, location shown in figure 10) indicating that these stands have been planted between 2007 and 2010. As the backscatter and optical signal of palms and forest are expected to mix-up, and the role of tree crops regarding the forest definition hasn't been settled yet, coconut stands have to be delineated separately using very-high resolution (VHR) optical data.

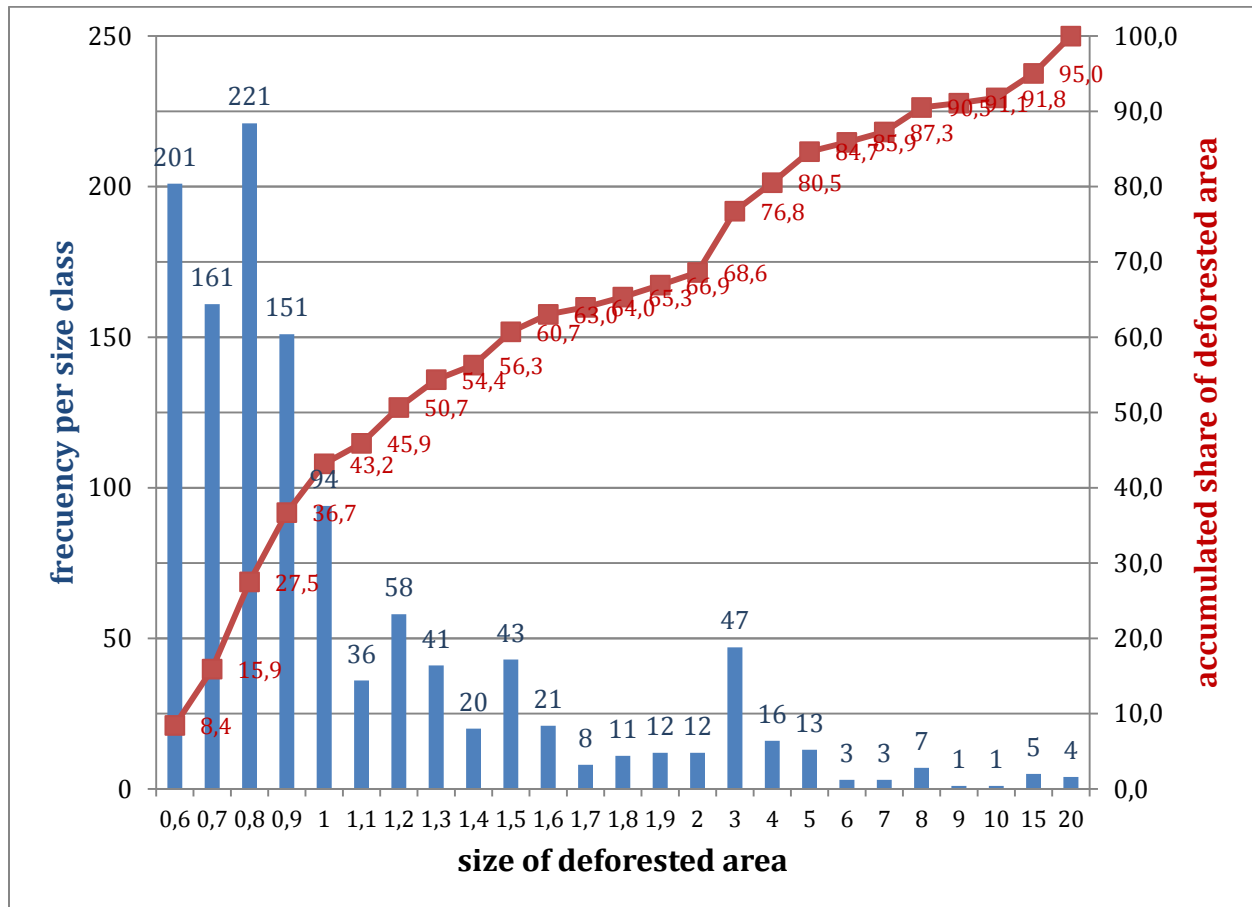
Figure 12 reveals another important aspect. The radar derived land mask (red) doesn't fit to the coastline based on the 5m DSM (yellow), or to the coastline visible in the WorldView 2 scene. Discrepancies between the boundaries derived from three different sources can be observed along the West coast, too, and have to be addressed in the accuracy assessment.

The histogram of the size of deforested area (figure 13) reveals, most of the deforestation is driven by small scale activities: Areas smaller than 1.3 ha contribute to 50.7% of the total deforestation in 2007-2010, while 21 areas larger than 6 ha contribute to 20% of total deforestation.

Figure 13: Histogram of the size of deforested areas during 2007-2010

Figure 12: Deforestation pattern in the Southwest over WorldView-2 band 7-5-2 scene (2011)





Step 10: Accuracy Assessment

The pattern assessment already revealed certain geo-location errors when comparing the shoreline derived by different sources. Although the ALOS Palsar K&C3 mosaic data was ortho-rectified using the SRTM 90m DSM, its geo-location error appears high (100-200m) when comparing its land boundary with the shorelines derived from WorldView2 data or the 5m DSM. These errors need to be addressed before assessing the thematic accuracy. In case of islands, the shoreline itself can't be considered a reliable reference as it shifts due to tidal change. To establish a common reference, suitable ground control points (GCPs) need to be identified in the different data sets to be collected in the field using GPS. In any event, it is important to improve the ortho-rectification and registration of SAR data. The first task can be achieved in two ways: Either the SAR tiles (step 2) are geo-referenced to a suitable source. As Vanuatu counts with a VHR DSM and WorldView-2 data, the data set, which fits best to the GCPs collected in the field. Or raw Level 1.1 ALOS Palsar data has to be requested from JAXA⁶ to be geocoded⁷ process using the VHR DSM. The second tasks refers to

⁶ The current agreement between GIZ and JAXA covers additional data request.

⁷ NEST 4C-1.1 provides geocoding functionality.

registering the ALOS Palsar tiles to the data used in assessing Vanuatu's historic deforestation patterns (Herold et al. 2007) or vice versa.

A second challenge for the accuracy assessment is the deforestation pattern itself. The change pattern generated here does not provide a reliable forest-/non-forest mask for the initial year (2007). Thus, while the detected changes for the reporting period (e.g. those visible in figure 11) coincide with no-forest in 2011, there is no certainty, that these areas have been covered by forest in 2007. A thorough accuracy assessment would require assessing the detection of the initial state of the forest (forest cover map 2007) and the detected changes within the forest domain at the end of the reporting period (2010 forest-/non-forest-/deforestation map) using higher resolution verification sources. To fulfill this task, land use and land cover in 2007 would have to be classified⁸, which goes beyond this processing chain.

Once the geo-reference of the SAR tiles has been improved and the deforestation pattern has been complemented processing a 2007 (or 2010) forest-/non-forest map a sampling design for the accuracy assessment can be developed. Developing and unaligned systematic random sampling scheme might be a good option. A square segment area frame sampling approach can be used covering the land mask with square blocks within a regular grid (Gallego 1995). Each block is divided into an equal number of segments, of which a predefined number of segments is randomly selected. GME (cf. footnote 4) provides the tools to develop such a scheme. The segments can be visually interpreted comparing the land cover (change) with (V)HR data to calculate the producer accuracy (error of omission) , the user accuracy (error of commission⁹) and the overall accuracy using a confusion matrix (Strahler et al. 2006). Annex 3 illustrates the sampling design.

5. Recommendations to improve the processing chain

The results of the ALOS Palsar K&C3 mosaic processing indicate that Santo Island lost 1,396.8 ha of forests or 465.6 ha/yr over a period of 3 years (2007-2010). This implies that the annual deforestation rate is five times higher compared to the period 1990-2000¹⁰, with more than 50% of the deforestation being driven by small-scale interventions converting less than 1.3 ha in 3 years. Obviously, the results require a thorough accuracy assessment. Besides, there is room for improving the processing chain.

⁸ JAXA's K&C3 Training package provides a software tool for land use / land cover classification of SAR data applying image segmentation.

⁹ An error of omission occurs, if a case is not assigned to the class it belongs. If it is assigned to class it doesn't belong to it is accounted as an error of commission.

¹⁰ According to data of Herold et al. (2007), Santo lost 990 ha of forest between 1990 and 2000. To assess the comparability of the results both methods would have to be applied to data covering the same period. Given the current data constraints, this appears impossible as Landsat didn't cover Vanuatu well during the last ten years.

First, the missing scene S14E167 covering Santo's northeast has to be acquired and processed. In case the scene can't be made available, cloud-free Landsat 7 ETM data covering this part without SLC-error gaps is available in the USGS archive¹¹.

The SAR processing reduced the extent of areas remaining unclassified. While the results of the optical processing chain for 1990-2000 showed left 5.6% of the area unclassified due to clouds and shadows, the ALOS Palsar mosaic processing had to exclude 3.1 % due to radiometric and geometric distortions (FLS). This share can be reduced easily classifying the remaining distorted area using VHR data¹². Apart, the FLS distortions can be reduced processing ALOS Palsar Level 1.1 data to be geocode with Vanuatu's VHR DSM. Furthermore, SAR data acquired from different side-looking angles can be included which reduces the FLS distortions, too.

To reduce seasonality effect, particularly soil moisture variability over canopies, available for 2008 and 2009 data can be processed additionally. To improve the thematic accuracy, annual forest-/non-forest masks for 2007, 2008, 2009, and 2010 should be generated using JAXA's segmentation and classification tool. Once the processing has been improved, a thorough accuracy assessment can be conducted leading eventually to an adjustment of processing parameters (average forest HV backscatter, user-defined thresholds).

Going beyond the mere improvement of the SAR processing chains, the optical and the radar- based processing chain have to be linked in a way, that the detected deforestation rates and forest-non-forest maps for different periods (1990-2000, 2007-2010) are comparable in terms of their thematic and geometric accuracy. The cross calibration is necessary to derive the deforestation rate for the period 2000-2007. As L-Band SAR data isn't available for that period, and only a very few and highly fragmented Landsat 7 ETM scenes, as well as few SPOT and ASTER scenes cover Vanuatu, the cross calibration can be carried out only across a limited calibration site. The cross calibration would build on the deforestation pattern for 2000-2007 applying the methodology of Herold et al. (2007) to derive the forest-/non-forest map. Both, the optically derived and the SAR based 2007 forest map have to be validated using higher resolution imagery (Quickbird, Ikonos) for 2007 or 2008.

¹¹ The 3 scenes LE70820702010100EDC00 (10.04.2010), LE70820702008143EDC00 (22.05.2008), LE70820702007124EDC00 (04.05.2007) can be downloaded at <http://earthexplorer.usgs.gov/>.

¹² If the same data (e.g. WorldView-2 2011 scenes) are being used for classification and the accuracy assessment, the samples of the accuracy assessment shall not cover FLS distorted areas classified using the same data source.

References

- Beyer, H.L. 2012. "Geospatial Modelling Environment (Version 0.7.2.0)."
www.spatialecology.com/gme.
- Gallego, F. J. 1995. *Sampling frames of square segments*. Commission of the European Communities. Joint Research Centre.
- Herold, Martin, Jacqueline Sambale, Martin Lindner, Marcel Urban, and Sean Weaver. 2007. "Satellite Based Monitoring of the National Forest Resources in the Pacific Island State of Vanuatu. Proceedings of the Tri-National Conference 2007 of the Swiss, Austrian and German Society for Photogrammetry and Remote Sensing, 19.-21.06.2007, Basel/Switzerland, 319-328." In *Von Der Medizintechnik Bis Zur Planetenforschung – Photogrammetrie Und Fernerkundung Für Das 21. Jahrhundert. Vorträge Dreiländertagung 27. Wissenschaftlich-Technische Jahrestagung Der DGPF 19. – 21. Juni 2007 in Muttenz, Basel*. Vol. 16. Muttenz, Basel: Deutsche Gesellschaft für Photogrammetrie, Fernerkundung und Geoinformation e.V. DGFP.
- Isoguchi, Osamu. 2012. "Training of Forest Change Detection Using PALSAR Gamma Naught" November 5, RESTEC HQ Office.
- JAXA. 2008. "ALOS User Handbook." <http://www.eorc.jaxa.jp/ALOS/en/doc/handbk.htm>.
- . 2012a. "ALOS/PALSAR 25m Mosaic Product Format Description". Earth Observation Research Center.
- . 2012b. "KC18 and JAXA-REDD+ Material Training Course on ALOS PALSAR Mosaic Analysis for Forest Monitoring,"
- Lee, Jong-Sen, and Eric Pottier. 2009. *Polarimetric Radar Imaging: From Basics to Applications*. Optical Science and Engineering 142. Boca Raton: CRC Press.
- Leica Geosystems. 2006. "ERDAS IMAGINE®Tour Guides."
- Lusch, David. 1999. "Introduction to Microwave Remote Sensing". Center for Remote Sensing and Geographic Information Science, Michigan State University.
- Motohka, Takeshi. 2012. "Introduction on Forest Change Mapping Using PALSAR Gamma Naught Change" presented at the JAXA Training Course in KC#18, May 11, RESTEC HQ Office.
- Natural Resources Canada. 2007. "GlobeSAR-2 Radar Remote Sensing Training Package." <http://www.nrcan.gc.ca/earth-sciences/geography-boundary/remote-sensing/radar-remote/1108>.
- R Core Team. 2012. "R: A Language and Environment for Statistical Computing. R Foundation for Statistical Computing". Vienna. www.R-project.org.
- Shimada, Masanobu. 2010. "Ortho-Rectification and Slope Correction of SAR Data Using DEM and Its Accuracy Evaluation." *IEEE Journal of Selected Topics in Applied Earth Observations and Remote Sensing* 3 (4) (December): 657–671. doi:10.1109/JSTARS.2010.2072984.
- Strahler, Alan H., Luigi Boschetti, Giles M. Foody, Mark A. Friedl, Matthew C. Hansen, Martin Herold, Philippe Mayaux, Jeffrey T. Morisette, Stephen V. Stehman, and Curtis E. Woodcock. 2006. "Global Land Cover Validation: Recommendations for Evaluation and Accuracy Assessment of Global Land Cover Maps". Office for Official Publications of the European Communities.

Acronyms

CF	Calibration Factor
db	decibel
DN	Digital Numbers
DoF	Vanuatu Department of Forestry
DSM	Digital Surface Model
FBD	Fine resolution model dual polarization
FLS	Foreshortening, layover, range and azimuth shift, radiometric variation due to the slope, and radar shadowing
GCP	Ground control points
GOFC-GOLD	Global Observation of Forest and Land Cover Dynamics
IPCC	Intergovernmental Panel on Climate Change
JAXA	Japan Aerospace Exploration Agency
K&C3	3rd Kyoto and Carbon Science Program
LCC	Land cover change
LULUCF	Land Use, Land-Use Change, and Forestry
MMU	Minimum mapping unit
MRV	Measurement, reporting, and verification
NRCS	Normalized radar cross section
ORI	Orthorectified Radar Image
REDD+	Reducing emissions from deforestation, forest degradation, conservation, sustainable management of forests and enhancement of carbon stocks
RS	Remote sensing
SAR	Synthetic Aperture Radar (SAR)
SBSTA	Subsidiary Body on Scientific and Technological Advice
SRTM	Shuttle Radar Topography Mission
UNFCCC	United Nations Framework Convention on Climate Change
VHR	Very-high resolution (VHR) optical data
WGS	World Geodetic System

Annex 1: Header file content for tiles S15E166 and S15E67

The following headers provide the parameters for the HH, HV, and date files. For incidence angle and mask files data types (line 9) have to be set to "1".

S15E166_10_sl_HH

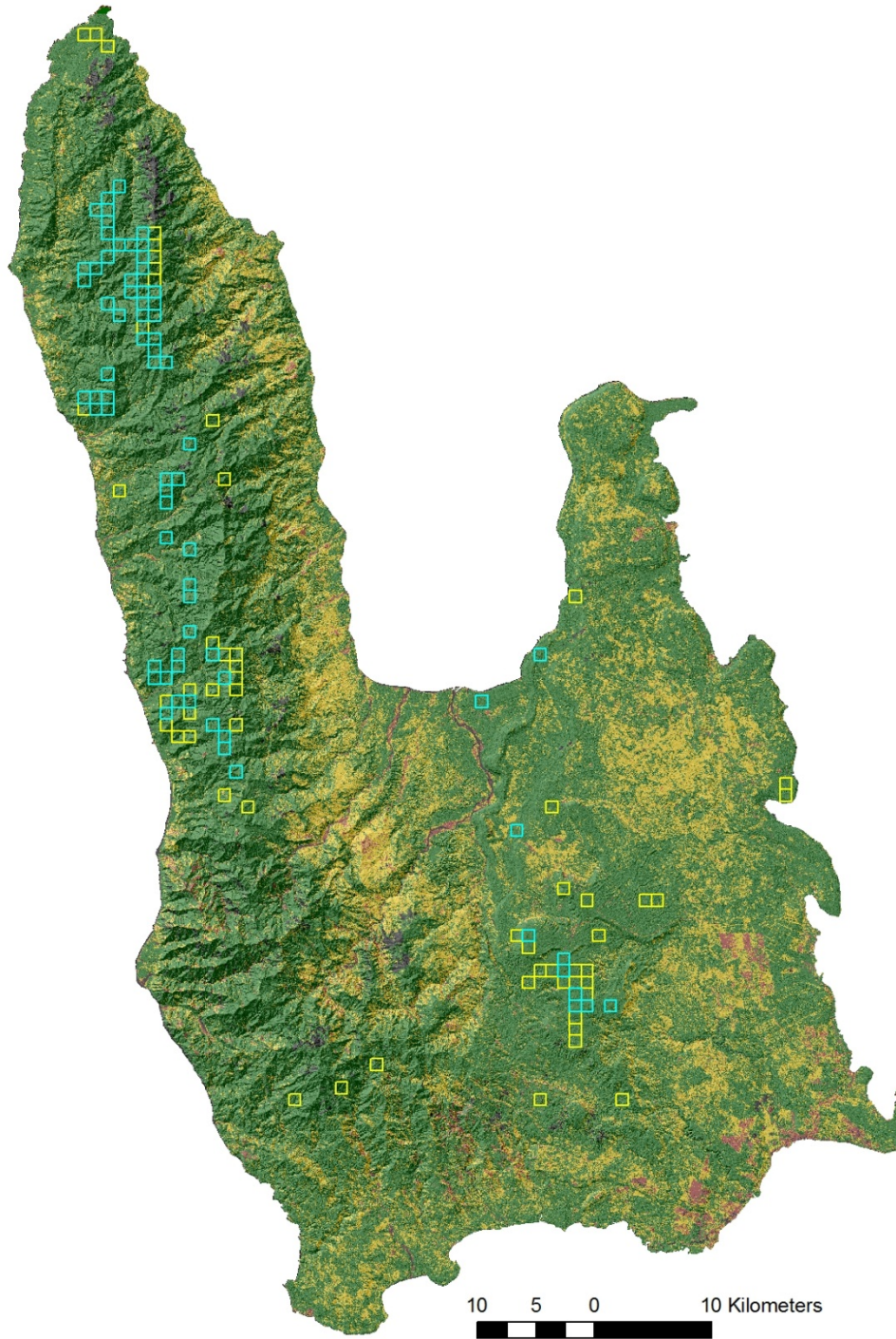
```
ENVI
description = {
  File Imported into ENVI.}
samples = 4500
lines = 4500
bands = 1
header offset = 0
file type = ENVI Standard
data type = 12
interleave = bsq
sensor type = Unknown
byte order = 0
map info = {Geographic Lat/Lon, 1.0000, 1.0000, 166.00000000, -15.00000000, 2.2222000000e-004,
2.2222000000e-004, WGS-84, units=Degrees}
coordinate system string =
{GEOGCS["GCS_WGS_1984",DATUM["D_WGS_1984",SPHEROID["WGS_1984",6378137.0,298.25722356
3]],PRIMEM["Greenwich",0.0],UNIT["Degree",0.0174532925199433]]}
wavelength units = Unknown
```

S15E167_10_sl_HH

```
ENVI
description = {
  File Imported into ENVI.}
samples = 4500
lines = 4500
bands = 1
header offset = 0
file type = ENVI Standard
data type = 12
interleave = bsq
sensor type = Unknown
byte order = 0
map info = {Geographic Lat/Lon, 1.0000, 1.0000, 167.00000000, -15.00000000, 2.2222000000e-004,
2.2222000000e-004, WGS-84, units=Degrees}
coordinate system string =
{GEOGCS["GCS_WGS_1984",DATUM["D_WGS_1984",SPHEROID["WGS_1984",6378137.0,298.25722356
3]],PRIMEM["Greenwich",0.0],UNIT["Degree",0.0174532925199433]]}
wavelength units = Unknown
```

Annex 2: HV forest sampling design

2011-samples completely covered with forest (cyan) overlaid over 2000 forest/non-forest mask (forest: green, woodlands: yellow, bare soil: brown (Herold et al. 2007)).



Annex 3: Accuracy assessment sampling design

The following unaligned systematic random sampling scheme implemented as a square segment area frame sampling approach has been developed using the *genregionsampleplots* command in GME (frame size: 8km x 8km; segment size: 800m x 800 m). 3 segments per frame were randomly selected calling the *r.sample* command of R (R Core Team 2012) from GME leading to a sample size of 267 segments.

